A study of the magnetoresistance of the charge-transfer salt $(BEDT-TTF)_3Cl_2 \cdot 2H_2O$ at hydrostatic pressures of up to 20 kbar: evidence for a charge-density-wave ground state and the observation of pressure-induced superconductivity

1996 J. Phys.: Condens. Matter 8 6005

(http://iopscience.iop.org/0953-8984/8/33/009)

J. Phys.: Condens. Matter **8** (1996) 6005–6017. Printed in the UK

A study of the magnetoresistance of the charge-transfer salt (BEDT-TTF)$_3$Cl$_2 \cdot 2$H$_2$O at hydrostatic pressures of up to 20 kbar: evidence for a charge-density-wave ground state and the observation of pressure-induced superconductivity

W Lubczynski†‡, S V Demishev†§, J Singleton†, J M Caulfield†, L du Croo de Jongh†, C J Kepert‖, S J Blundell†, W Hayes†, M Kurmoo‖ and P Day‖

† Department of Physics, University of Oxford, Clarendon Laboratory, Oxford OX1 3PU, UK
‡ Department of Solid State Physics, 41-800 Zabrze, Kalwalca 3, Poland
§ General Physics Institute, Vavilov Street 38, 117942 Moscow, Russia
‖ Royal Institution, 21 Albemarle Street, London W1X 4BS, UK

Received 9 January 1996, in final form 4 June 1996

Abstract. The magnetoresistance of single crystals of the quasi-two-dimensional (Q2D) organic conductor (BEDT-TTF)$_3$Cl$_2 \cdot 2$H$_2$O has been studied at temperatures between 700 mK and 300 K in magnetic fields of up to 15 T and hydrostatic pressures of up to 20 kbar. Measurements of the resistivity using a direct-current van der Pauw technique at ambient pressure show that the material undergoes a metal-to-insulator transition at ∼150 K; below this temperature the resistivity increases by more than five orders of magnitude as the samples are cooled to 4.2 K. If the current exceeds a critical value, the sample resistivity undergoes irreversible changes, and exhibits non-ohmic behaviour over a wide temperature range. Below 30 K, either an abrupt increase of the resistivity by two orders of magnitude or bistable behaviour is observed, depending on the size and/or direction of the measurement current and the sample history. These experimental data strongly suggest that the metal–insulator transition and complex resistivity behaviour are due to the formation of a charge-density wave (CDW) with a well-developed domain structure. The magnetotransport data recorded under hydrostatic pressure indicate that pressure has the effect of gradually reducing the CDW ordering temperature. At higher pressures, there is a pressure-induced transition from the CDW state to a metallic, superconducting state which occurs in two distinct stages. Firstly, a relatively small number of Q2D carriers are induced, evidence for which is seen in the form of the magnetoresistance and the presence of Shubnikov–de Haas oscillations; in spite of the low carrier density, the material then superconducts below a temperature of ∼2–3 K. Subsequently, at higher pressures, the CDW state collapses, resulting in Q1D behaviour of the magnetoresistance, and eventual suppression of the superconductivity.

1. Introduction

Charge-transfer salts of the molecule bis(ethylene-dithio)tetrathiafulvalene (BEDT-TTF) have been the focus of much attention over the last decade (see, e.g., reference [1] and references therein). The salts often have quasi-two-dimensional (Q2D) metallic properties, and can exhibit phenomena such as superconductivity, spin-density-wave (SDW) formation and magnetic-field-induced phase transitions [1]. Furthermore, the materials are relatively 'clean' systems, so their Fermi surfaces may be characterized using the

0953-8984/96/336005+13$19.50

Shubnikov–de Haas (e.g., reference [2] and references therein) and de Haas–van Alphen effects (e.g., reference [3] and references therein). Amongst this family the salt (BEDT-TTF)$_3$Cl$_2$ · 2H$_2$O is relatively unusual in that the BEDT-TTF ions have average charge $+\frac{2}{3}e$ [4, 5], instead of the more common $+\frac{1}{2}e$ [1]. Thermopower, susceptibility and conductivity measurements [7, 8] suggest that (BEDT-TTF)$_3$Cl$_2$·2H$_2$O is a semimetal at 300 K; at $T \approx 150$ K it undergoes a (semi)metal–insulator transition (MIT) [9]. The authors of reference [7] attributed the MIT to removal of the band overlap at low temperatures; however, in almost all other similar organic conductors MITs are believed to be connected with charge-density-wave (CDW) or SDW formation [7]. The application of hydrostatic pressure gradually reduces the onset temperature of the MIT and eventually stabilizes a superconducting state between 10.2 kbar and 13.5 kbar with $T_c \leqslant 4$ K [10, 11].

In this work we have attempted to clarify the origin of the phenomena described above. Absolute measurements of the resistivity at ambient pressure demonstrate that it is non-ohmic in nature at temperatures below the MIT, strongly suggesting that the MIT is caused by a CDW with well-developed domain structure at low temperatures. In addition, high magnetic fields and low temperatures have been employed to observe the Shubnikov–de Haas effect in (BEDT-TTF)$_3$Cl$_2$ · 2H$_2$O under high hydrostatic pressures. In this way properties of a closed Q2D section of the Fermi surface have been observed whilst pressure has been used to tune the material through the superconducting part of its phase diagram.

This paper is organized as follows: section 2 gives details of the experimental apparatus and a brief introduction to the properties, crystal structure and Fermi surface of (BEDT-TTF)$_3$Cl$_2$ · 2H$_2$O. Section 3 describes the experimental evidence which indicates that the MIT observed at ambient pressure is due to a CDW. Section 4 covers the high-pressure magnetoresistance measurements and presents a pressure–temperature phase diagram for (BEDT-TTF)$_3$Cl$_2$ · 2H$_2$O. A summary is given in section 5.

2. Sample properties and experimental details

2.1. General properties of (BEDT-TTF)$_3$Cl$_2$ · 2H$_2$O

(BEDT-TTF)$_3$Cl$_2$ · 2H$_2$O crystallizes in the triclinic space group $P\bar{1}$ with a unit-cell volume of 2.304 nm^3 [12]. The structure consists of sheets of BEDT-TTF molecules separated by layers of the anions; the unit cell contains slipped stacks of three crystallographically independent BEDT-TTF molecules, and there are two formula units per unit cell. All of the BEDT-TTF molecules are oriented approximately parallel to one another. On lowering the temperature the lattice contracts anisotropically [4].

The calculated Fermi surface of (BEDT-TTF)$_3$Cl$_2$ · 2H$_2$O consists of two parallel quasi-one-dimensional (Q1D) sections and an elongated closed electron pocket (e.g., reference [7] gives such a calculation; however, see also reference [5]); the transport properties are quasi-two-dimensional (Q2D) in character, with the ratio of the room temperature resistivities along the crystal axes a, b and c being ρ_a:ρ_b:ρ_c = 1:7:1000 [7, 9].

The high-purity single crystals of (BEDT-TTF)$_3$Cl$_2$ · 2H$_2$O used in this paper were prepared electrochemically using a technique described elsewhere [12]. The crystals are generally $\sim 2 \times 2 \times 0.05$ mm^3 black distorted hexagonal platelets with a metallic lustre, with the plane of the plate corresponding to the highly conducting Q2D layers.

2.2. Ambient pressure experiments

The ambient pressure resistivity measurements discussed in section 3 were performed on single crystals of (BEDT-TTF)$_3$Cl$_2 \cdot 2$H$_2$O using a direct current (DC) van der Pauw (VdP) method. Evaporated gold contacts were located around the perimeter of the samples and fine gold wires were attached to these using silver epoxy. The sample under study was supported in the cryostat by its wires alone in order to minimize stress, and good thermal contact with the thermometry was ensured by immersing the sample in low-pressure helium exchange gas. The temperature was varied in the range 4.2 K $\leqslant T \leqslant$ 300 K and magnetic fields of up to 14 T were applied to the sample using a superconductive magnet. Using such an arrangement samples withstood many cycles of cooling–heating without significant degradation of the contact quality.

With an anisotropic sample, the VdP method gives the value

$$\rho = (\rho_a \rho_b)^{1/2} = (R_a + R_b) f\left(\frac{R_a}{R_b}\right) d \tag{1}$$

where R_a and R_b are the VdP partial resistivities for the different measuring current (I) directions in the sample, d denotes the sample thickness and the function $f(R_a/R_b)$ takes into account the current path distribution in the sample [13]. In the present case the contact geometry was such that R_a and R_b corresponded to current directions approximately parallel to the a and b crystal axes. Measurements of the R_a- and R_b-values were performed for two DC current polarities in order to eliminate thermoelectric contributions from the contacts and wiring.

2.3. Measurements at high hydrostatic pressures

(BEDT-TTF)$_3$Cl$_2 \cdot 2$H$_2$O single crystals from the same batch as those used in the ambient pressure measurements were selected for study at high hydrostatic pressures (section 4). Electrical contacts were attached to previously evaporated gold pads on both sample faces using silver epoxy, resulting in contact resistances of less than 10 Ω per pair at 300 K. As the hydrostatic pressure experiments involved temperatures down to 700 mK, standard four-wire alternating current (AC) techniques (5–150 Hz) were employed; thus, a reasonable signal-to-noise ratio was achieved even though the sample currents were much lower than those used in the DC VdP techniques described above. The current was applied in the ab-plane of the crystal platelet; great care was taken to ensure that the currents used did not cause sample heating and did not result in irreversible changes to the sample behaviour (see section 3). The magnetic field was applied in the c^*-direction, perpendicular to the Q2D planes.

Magnetoresistance measurements under hydrostatic pressure were carried out using a non-magnetic clamp cell filled with a petroleum spirit pressure medium [14]. The cell used for the majority of the experiments provides pressures of up to 16.5 kbar at liquid helium temperatures. Pressure was applied at room temperature using a hydraulic press, after which the cell was placed in a specially designed ^{3}He cryostat providing temperatures down to 700 mK in a 15 T superconducting magnet; cooling from room temperature to 4.2 K was accomplished over a period of around 12 hours to ensure that the pressure was ideally hydrostatic at low temperatures. For pressures between 16.5 kbar and 20 kbar the sample was transferred to a larger clamp cell; such measurements were limited to pumped ^{4}He temperatures as the cell was too large for the ^{3}He cryostat. The temperature of the sample was measured using a calibrated ruthenium oxide sensor, and the pressure in the cell at all temperatures was monitored using the resistance of manganin wire with a known

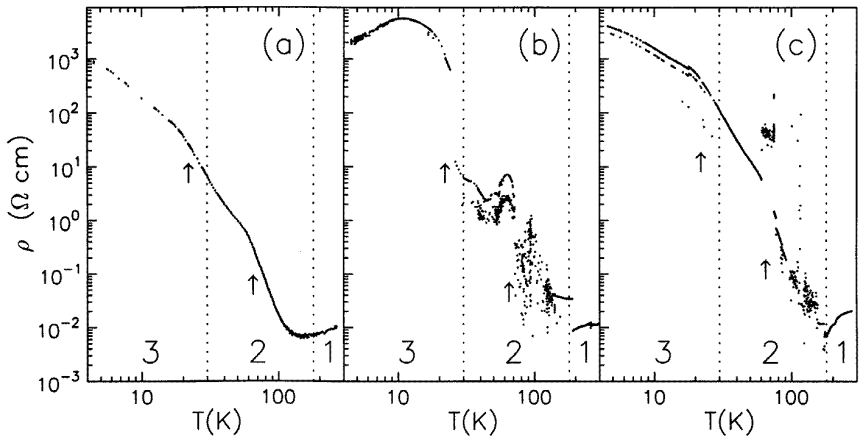

Figure 1. Temperature dependence of the resistivity in (BEDT-TTF)$_3$Cl$_2 \cdot 2$H$_2$O measured by the Van der Pauw method for different measurement currents I and sample states (see the text for details). (a) $I = 1$ μA, sample in the initial state; (b) $I = 1$ μA, after heating and cooling cycles under higher current; (c) $I = 10$ μA. The arrows indicate the positions of the 'kinks' in the resistivity and regions 1, 2 and 3 delineate different types of behaviour (see the text).

pressure and temperature coefficient. All of the pressures quoted in section 4 are those measured at 4.2 K and all of the data shown in the figures of section 4 are for the same (BEDT-TTF)$_3$Cl$_2 \cdot 2$H$_2$O sample for ease of comparison.

3. Evidence for a CDW ground state at ambient pressure

3.1. Ambient pressure resistivity measurements

The measured temperature dependence of the resistivity $\rho(T)$ of (BEDT-TTF)$_3$Cl$_2 \cdot 2$H$_2$O was found to depend strongly on the value of the measuring current I and the route by which the sample reached the particular temperature; typical data are shown in figure 1. When I is less than 1 μA the $\rho(T)$-curve is very similar to that obtained in reference [7] using AC techniques; the resistivity first decreases as the temperature is lowered, and then in the region where $T \lesssim 150$ K it increases by more than five orders of magnitude as the sample is cooled to 4.2 K (figure 1(a)). (Note that figure 1 shows *absolute* values of the resistivity, in contrast to the 'arbitrary units' of the data reported in reference [7].)

An increase in the measuring current to $I = 10$ μA leads to irreversible changes in the form of the $\rho(T)$-curves; the data in figure 1(b) illustrate the effect of measuring the resistivity of the (BEDT-TTF)$_3$Cl$_2 \cdot 2$H$_2$O sample using $I = 1$ μA after it has been cooled and warmed with $I = 10$ μA flowing. Three characteristic regions with differing behaviour can be seen. For temperatures $T > T_{\mathrm{MIT}} \approx 150$ K (labelled region 1 in figure 1), $\rho(T)$ decreases as T is lowered. However, for $T < T_{\mathrm{MIT}}$, the behaviour of $\rho(T)$ becomes non-ohmic and non-single-valued and this persists down to $T \approx 30$–40 K (the range of non-ohmic behaviour is labelled region 2 in figure 1). Below $T \approx 30$–40 K (region 3 in figure 1) the relationship between ρ and T becomes single-valued once more. Close to the boundary between regions 2 and 3 ρ jumps by two orders of magnitude (figure 1(b)). As the temperature is lowered further, $\rho(T)$ increases more slowly before beginning to saturate below $T \approx 8$ K.

Once the (BEDT-TTF)$_3$Cl$_2 \cdot 2$H$_2$O sample is in the new state resulting from cooling under $I = 10\ \mu$A, increases of I do not appear to change the qualitative behaviour of $\rho(T)$ in regions 1 and 2 of figure 1, but do result in larger variation in ρ; an example of this is shown in figure 1(c) with $I = 10\ \mu$A. Here we observe two well-defined 'branches' between which the resistivity switches. This bistability was also observed up to currents of $100\ \mu$A (not shown). These measurements required very low rates of temperature variation (typically $\leqslant 1$ K min^{-1}).

The behaviour of $\rho(T)$ shown in figure 1 is reasonably reproducible for both cooling and heating cycles and amongst different (BEDT-TTF)$_3$Cl$_2 \cdot 2$H$_2$O samples. Particular care was taken to check that the contacts had not degraded with thermal cycling (see section 2). However, the low-temperature bistability (region 3) and the instabilities in region 2 were found to be sensitive to the alteration of the current direction required by the VdP method. If the current commutation was switched off, so that only R_a or R_b were measured, their temperature dependence became single-valued and non-fluctuating.

Previous workers [7] have noted the presence of various 'kinks' in the ρ–T-curves of (BEDT-TTF)$_3$Cl$_2 \cdot 2$H$_2$O and these were also observed for the present samples in their initial state (figure 1(a), arrows). There is some correlation between the temperatures at which the kinks on the $\rho(T)$-curve for the initial sample state are seen with the characteristic features of the unstable curves (figure 1(b) and (c), arrows).

The resistivity measurements in the low-temperature region (region 3) were repeated with the (BEDT-TTF)$_3$Cl$_2 \cdot 2$H$_2$O samples in magnetic fields B of up to 14 T. It was found that ρ increased smoothly with B, growing to $\sim$1.3 times its zero-field value at 14 T. No sharp features were observed in the magnetoresistance, $\rho(B)$, even at the very lowest temperatures ($\sim$4 K). In general, $\rho(B)$ can consist of several branches depending on the current direction; removal of the commutation required by the VdP method always leads to the survival of only one branch.

3.2. Discussion

The results in figure 1 can be explained by assuming that the ground state involves a CDW. Below 150 K the long-range order may develop but be frustrated by pinning. This frustration is removed at temperatures below $\sim$30–40 K where the CDW may couple much more effectively to the underlying lattice. An alternative way to explain the three regions of differing behaviour in figure 1 is to suggest that the CDW formation may involve two steps [15] in which partial ordering initially occurs at high temperature along the 'easy' direction defined by the stronger one-dimensional correlations; at a lower temperature full ordering occurs along the perpendicular direction. In this interpretation the intermediate-temperature regime (region 2 in figure 1) is partially ordered and may be associated with non-single-valued behaviour. The switching of the current direction in this region may induce additional complex behaviour because of the interaction between the external electric field and locally ordered regions in the sample which are pinned to lattice defects (see below).

In either interpretation, the low-temperature ground state may be further complicated by the formation of fixed domain structure [16]. The presence of bistability and non-ohmic behaviour in ρ at higher currents in region 3 (figure 1(c)) can then be explained by the alteration of the domain structure by the electric field or by sliding of the density wave. Either process will result in changes in the current paths and hence the measured resistivity.

In such a model for the behaviour of (BEDT-TTF)$_3$Cl$_2 \cdot 2$H$_2$O, some form of density wave pinning is essential to explain the resistivity in regions 2 and 3 of figure 1. The role of cooling–heating cycles with currents $I \sim 10\ \mu$A and above is probably to produce

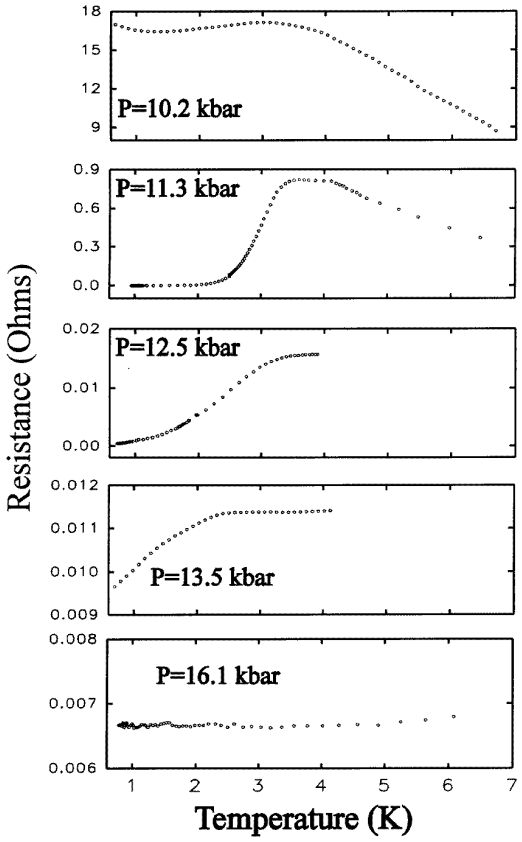

Figure 2. The measured resistance versus temperature (0.7–7 K) for a single crystal of (BEDT-TTF)$_3$Cl$_2 \cdot 2$H$_2$O at five different hydrostatic pressures.

structural defects in the sample; the fact that the resistivity always increases after such a cycle provides support for such an interpretation. These defects may act as the centres for density wave pinning and/or domain formation in region 3 of figure 1 and nuclei for the creation of locally ordered regions in region 2 of figure 1. The initial cooling curve for the sample at low currents (figure 1(a)) may therefore correspond to monodomain structure; in this case, the density wave formation just leads to bends in $\rho(T)$ rather than vertical jumps. Similar behaviour has been observed in other CDW systems [15].

The data in this section suggest that the density wave state in (BEDT-TTF)$_3$Cl$_2 \cdot 2$H$_2$O is much more likely to be a CDW rather than a SDW. In a SDW, spatial charge modulation is absent [15], so strong pinning effects and non-linear current–voltage characteristics such as those observed in regions 2 and 3 of figure 1 are less likely to occur. Secondly, magnetic fields of up to 14 T do not cause any distinctive features in the magnetoresistance. In the case of a SDW the ground state is antiferromagnetic; BEDT-TTF and TMTSF charge-transfer salts which are thought to possess SDW ground states often exhibit dramatic features in their low-temperature magnetoresistance which are interpreted as field-induced reorganizations of the SDW [18, 19, 20].

Additional evidence that the postulated density wave state is a CDW rather than a SDW is presented in figure 2 of reference [8], which shows the magnetic susceptibility of

(BEDT-TTF)$_3$Cl$_2 \cdot 2$H$_2$O as a function of temperature. As the temperature is lowered, the susceptibility falls smoothly to a very low value at $T \sim 80$ K and then remains small for further decreases in temperature; this behaviour is very different from the antiferromagnetic susceptibility characteristic of a SDW state [21].

Further evidence for the CDW has been found through a recent x-ray diffraction study at the European Synchrotron Radiation Facility [6]. In this experiment a single crystal was mounted inside a displex continuous-flow cryostat on Beamline 2 (ID11), and data were collected using 5° oscillations in ϕ and a wavelength of 0.07 nm. Sharp satellite reflections were seen at low temperatures, having intensities typically three to four orders of magnitude smaller than those of the neighbouring Bragg peaks. The satellite peaks indicate the presence of a long-range structural modulation in (BEDT-TTF)$_3$Cl$_2 \cdot 2$H$_2$O, characteristic of a Peierls distortion accompanying the formation of a three-dimensionally ordered CDW [6, 22].

In summary, all of the data described in this section strongly suggest that the MIT observed in (BEDT-TTF)$_3$Cl$_2 \cdot 2$H$_2$O is due to the formation of a CDW ground state, probably due to nesting of Q1D sections of the Fermi surface. In the next section the destruction of the proposed CDW by applied hydrostatic pressure will be examined.

4. Magnetoresistance measurements at high hydrostatic pressures

4.1. Experimental data

Measurements of the resistivity as the samples were cooling under hydrostatic pressure indicate that the MIT in (BEDT-TTF)$_3$Cl$_2 \cdot 2$H$_2$O is gradually suppressed by increasing pressure; e.g. at 11.3 kbar the resistivity has a minimum around 50 K (c.f. ∼150 K at ambient pressure (figure 1)), followed by a thirty-fold increase to a maximum at 3.5 K and then another rapid decrease. Once the pressure has reached 12.5 kbar and above, the minimum in resistivity is no longer observable. Such behaviour has previously been described in references [10, 11] (see sections 1 and 2) and so this section focuses on the low-temperature magnetoresistance of (BEDT-TTF)$_3$Cl$_2 \cdot 2$H$_2$O under pressure, which has not thus far been studied in detail.

Figure 2 shows the temperature dependence of the resistance of a single crystal of (BEDT-TTF)$_3$Cl$_2 \cdot 2$H$_2$O at five hydrostatic pressures in the low-temperature regime. Between 10.2 kbar and 12.5 kbar the resistivity at 3 K drops by almost three orders of magnitude. At the four lowest pressures shown in figure 2, there is a marked drop in the resistance at the very lowest temperatures, which is suppressed by the application of a magnetic field (figure 3). For the 11.3 kbar and 12.5 kbar data this behaviour is characteristic of full superconductivity. However, at 10.2 kbar there appears to be only a tendency to superconductivity (at ≈3 K). At this pressure zero resistance is not actually attained down to 0.7 K; nevertheless, the onset of this lowering in resistance is suppressed by the application of magnetic fields in a fashion characteristic of superconductivity. Similar behaviour (i.e. non-zero resistance in a superconducting state) has been observed in other BEDT-TTF salts [23] and high-T_c superconductors [24], and has been attributed in the latter materials to a Bose glass state [24].

The superconducting transition temperature (T_c), defined in this work as the point at which the resistance is 95% of its extrapolated normal-state value, increases with pressure, peaking at $T_c \approx 3.6$ K (figure 3, inset) under a pressure $p \approx 11.3$ kbar. Further increases in pressure cause T_c to decrease, until at $p \approx 14.5$ kbar the onset of superconductivity is not observable at temperatures above 0.7 K.

The magnetoresistance of a single crystal of (BEDT-TTF)$_3$Cl$_2 \cdot 2$H$_2$O is shown in

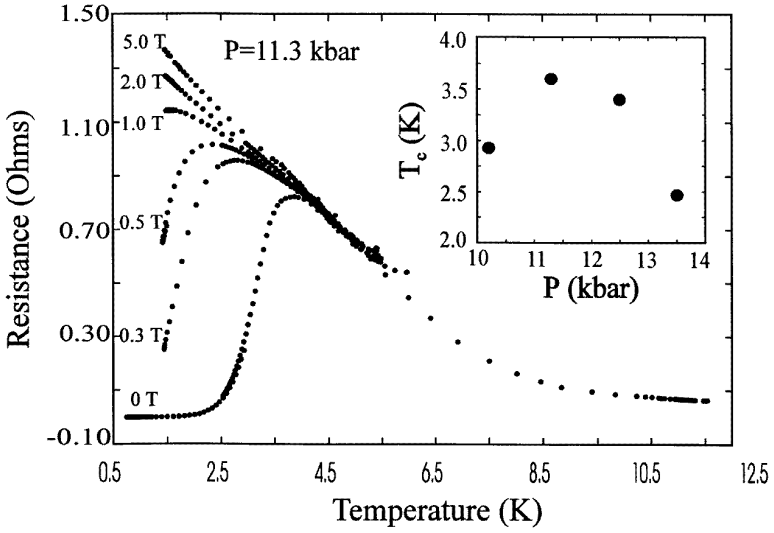

Figure 3. The suppression of superconductivity in (BEDT-TTF)$_3$Cl$_2$ · 2H$_2$O at 11.3 kbar using a magnetic field. The inset is a plot of T_c (i.e. the measured resistive onset (95% of the normal-resistance point) to superconductivity) versus pressure.

figure 4 for several applied hydrostatic pressures between 10.2 and 20 kbar at a temperature of 700 mK. At 10.2 and 11.3 kbar, the magnetoresistance saturates quickly, indicating that the Fermi surface is predominantly Q2D in character [25, 26]. However, as the pressure is increased to 12.5 kbar and above, the magnetoresistance changes form and no longer saturates within the available field range, indicating that the Fermi surface is now predominantly Q1D (open); i.e. the magnetic field is no longer effective in frustrating the ability of electrons to acquire energy from the driving electric field [25].

The ∼1000-fold drop in low-temperature magnetoresistance between 10.2 and 12.5 kbar, plus the non-observation of the resistance minimum at 12.5 kbar and above suggest that the CDW is completely destroyed by pressures of ∼12 kbar and above. As has been mentioned above, the CDW is probably due to nesting of Q1D Fermi surface sections; as a result of the destruction of the CDW, these Q1D sections will be able to contribute to the low-temperature magnetoresistance, leading to the observed non-saturating behaviour. The large change in resistance on destruction of the CDW suggests that the number of Q1D carriers thus free is much greater than the number of Q2D carriers contributing to the magnetoresistance at lower pressures (see below).

In spite of the non-saturating magnetoresistance at high pressures, evidence that at least one closed, Q2D section of Fermi surface remains above 12.5 kbar is observed as a single series of low-frequency oscillations superimposed on the magnetoresistance (figure 5). These oscillations are periodic in the reciprocal field (figure 5, inset) and possess all of the other attributes of Shubnikov–de Haas (SdH) oscillations [27]. We find no evidence for magnetic breakdown oscillations similar to those observed in the CDW state in $NbSe_3$ [28].

The frequency of the Shubnikov–de Haas oscillations due to the small Q2D pocket(s) increases with increasing pressure; rising from a value of 45 T at 12.5 kbar, it asymptotically approaches 100 T at 20 kbar (figure 6). These two frequency values correspond to orbits which have areas that are 1.7% and 3.8% of the total Brillouin zone area respectively. By fitting the temperature dependence of the Fourier amplitude of the magnetoresistance

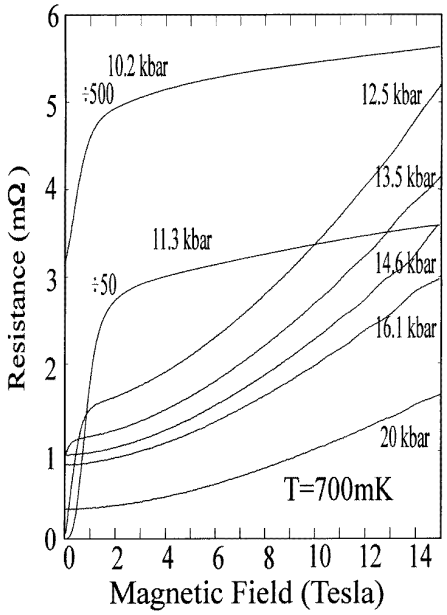

Figure 4. The magnetoresistance of (BEDT-TTF)$_3$Cl$_2 \cdot 2$H$_2$O at 0.7 K (the magnetic field is applied perpendicular to the *ac*-plane) for seven different pressures between 10.2 and 20 kbar. All of the data are from the same sample; the resistance values for 10.2 kbar and 11.3 kbar have been divided by 500 and 50 respectively in order to make comparisons with the other data possible.

oscillations between 12 and 17 T to the Lifshitz–Kosevich formula [3, 25], an effective mass of $(0.80 \pm 0.1)m_e$ was obtained at 13.5 kbar; at 16.1 kbar the value obtained was $(0.75 \pm 0.1)m_e$. Unfortunately the quasiparticle scattering rate (i.e. Dingle temperature) [25] is difficult to measure as there are so few oscillations in the magnetic field range attainable, although the rate of increase in amplitude with field does not vary appreciably with pressure. The data therefore imply that the effective mass and scattering rate are not very pressure dependent within the errors, in contrast to those of other superconducting BEDT-TTF salts (see, e.g., reference [29]).

In summary, the data presented in this section imply that the pressure-induced suppression of the highly resistive CDW state occurs in two stages. First of all, the pressure causes a small number of Q2D carriers to appear; perhaps a band drops below the Fermi level, and so one or more small, Q2D pockets become populated. The material is then metallic, but with a relatively small conductivity. Subsequent increases in pressure suppress the CDW, closing the band gaps along the quasi-one-dimensional Fermi surface sections; hence, the resistivity falls further and the magnetoresistance assumes a non-saturating behaviour.

4.2. The phase diagram

Figure 7 shows a notional pressure–temperature phase diagram for (BEDT-TTF)$_3$Cl$_2 \cdot 2$H$_2$O, constructed using the data in this work. The upper boundary is formed by the minimum in resistivity observed close to 150 K at ambient pressure; in the discussion of section 3 this resistivity minimum was associated with T_1, the onset temperature for partial CDW

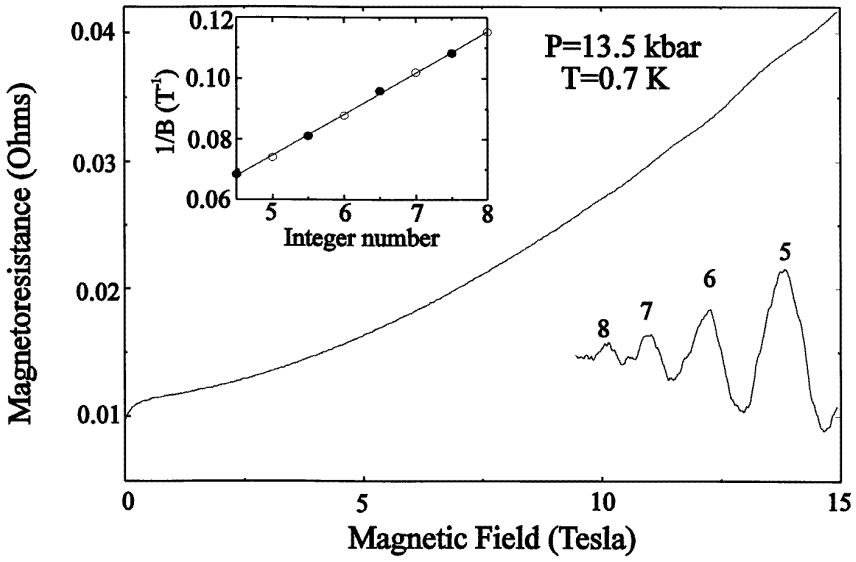

Figure 5. The magnetoresistance of (BEDT-TTF)$_3$Cl$_2$ · 2H$_2$O at 0.7 K (the magnetic field is applied perpendicular to the *ac*-plane) for a hydrostatic pressure of 13.5 kbar. The oscillatory component of the magnetoresistance after the removal of the slowly varying classical magnetoresistance is also shown. The inset is a plot of the oscillation position (in the reciprocal field) versus the Landau level index at 13.5 kbar. The solid line has a gradient of 74 T, filled dots correspond to magnetoresistance dips and open dots to magnetoresistance peaks.

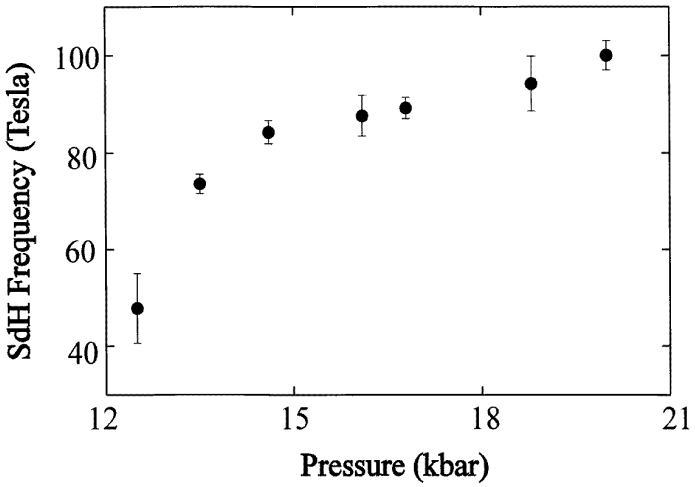

Figure 6. The measured Shubnikov–de Haas oscillation frequency plotted as a function of pressure.

order. Increases in pressure result in the resistivity minimum temperature T_1 decreasing; two additional data points from reference [11] (filled circles) have been included in order to delineate this boundary more clearly [30]. The temperature below which complete CDW order is established was only measured at ambient pressure; this point is shown as an ellipse

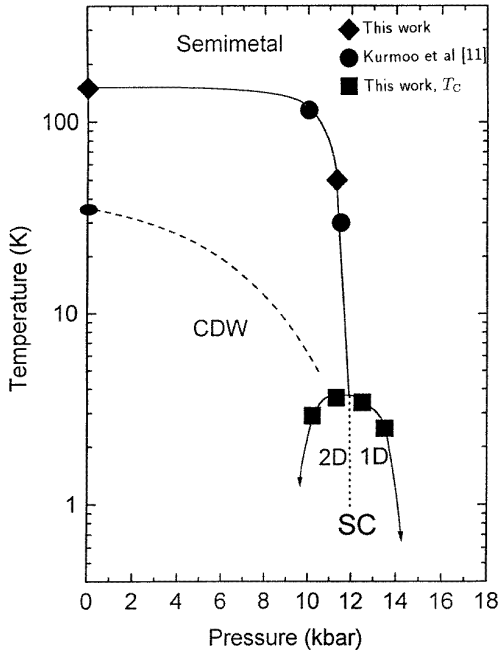

Figure 7. A temperature–pressure phase diagram: diamonds (this work) and circles (reference [11], pressures corrected to low-temperature values) represent the resistive minimum temperature. The solid ellipse indicates the ambient pressure temperature below which full CDW order is established (this work) and the dashed curve shows schematically its probable motion with pressure. The squares are the superconducting T_c (this work), and the dotted line divides the region of Q2D saturating magnetoresistance from that of Q1D non-saturating magnetoresistance. Other symbols: CDW = charge-density wave; SC = superconductor.

and the dashed line indicates schematically the probable lowering of this temperature with increasing pressure. The superconducting region is bounded by the T_c-values deduced using the 95% extrapolated normal-resistivity criterion. The vertical dotted line inside the superconducting region separates the Q2D saturating magnetoresistance behaviour from the Q1D.

A simpler phase diagram was also shown in reference [11]; once the pressures plotted in the latter work have been adjusted to low-temperature values [30], the phase diagram of reference [11] is in good agreement with figure 7. On the other hand, the resistivity minima temperatures shown in reference [10] appear offset by $\approx$3 kbar from the points in figure 7 at high pressures. A possible reason for this discrepancy is that the pressures quoted in reference [10] may be room temperature values (i.e. not adjusted for the loss in pressure experienced as the pressure cell is cooled); unfortunately this point is not clear from the text of reference [10]. Alternatively, the differences could result from different sample preparation methods or crystal purity.

The appearance of the saturating (Q2D) magnetoresistance and superconductivity at the same pressure indicates that the superconductivity is associated with the small number of Q2D carriers. Support for this view is given by the values of the coherence length ξ estimated from the rate of change of B_{c2} with temperature [26] ($\xi \approx 15$ nm at 11.3 kbar and $\xi \approx 17$ nm at 12.5 kbar), which are in good agreement with the value $\xi \approx 15$ nm obtained using $\xi = 0.18\bar{h}v_F/k_BT_c$, with v_F the mean Fermi velocity deduced from the Shubnikov–de

Haas frequency at 12.5 kbar [26].

Figure 7 shows that the superconducting part of the phase diagram is restricted to a small region close to the almost vertical drop in the phase boundary between the CDW and semimetallic regions. This suggests that the strong fluctuations which will occur close to such a boundary may form a vital part of the mechanism for superconductivity in (BEDT-TTF)$_3$Cl$_2$·2H$_2$O. Qualitatively similar behaviour has been observed in other superconducting systems; e.g. T_c peaks in $La_{2-x}Sr_xCuO_{4+y}$ close to the tetragonal–orthorhombic structural phase boundary [31] and reaches a maximum close to the boundary marking the fcc lattice instability in the non-equilibrium solid solutions $Al_{1-x}Si_x$ [32]. An alternative view has been proposed by Caulfield [26], who suggested that the superconducting state might be suppressed by screening of the pairing interaction by the Q1D carriers or that structural changes brought about by the application of pressure may lead to changes in the phonon spectrum which affect the formation of the superconducting state.

5. Summary

This paper has presented the results of resistivity and magnetoresistance experiments on single crystals of (BEDT-TTF)$_3$Cl$_2$ · 2H$_2$O, some involving pressures as high as 20 kbar. The ambient pressure magnetoresistance and x-ray data suggest that the (semi-)metal-to-insulator transition (MIT) and subsequent complex behaviour of the resistivity observed in (BEDT-TTF)$_3$Cl$_2$ · 2H$_2$O are due to the formation of a charge-density wave (CDW) with well-developed domain structure, probably caused by nesting of quasi-one-dimensional (Q1D) Fermi surface sections. Structural defects in the material, induced by high electric currents, seem to be important in pinning the CDW, and hence have a marked effect on the observed resistivity. The magnetotransport data recorded under hydrostatic pressure indicate that pressure has the effect of gradually reducing the CDW ordering temperature. However, rather than just representing the destruction of the CDW state, the pressure-induced transition from the semiconducting state observed at low temperatures and pressures appears to occur in two distinct stages; firstly, the pressure causes a closed Q2D Fermi surface section to form, and then subsequently the CDW state collapses, resulting in Q1D behaviour.

Acknowledgments

This work was supported by the EPSRC and the Royal Society (UK) and by the European Community HCM scheme. It was also funded in part by INTAS projects INTAS 93-2400 and INTAS 94-1788 and by the 'Fullerenes and atomic clusters' programme of the Russian Ministry of Science. WL is grateful to the Royal Society for the provision of a visiting fellowship for the duration of his stay in Oxford. The authors are grateful to Professor G Grüner and Professor P Monceau for helpful discussions and to the referees for some useful suggestions. We should also like to thank Dennis Rawlings, Terry Holiday, Nickolay Samarin, Nickolay Sluchanko and M V Kondrin for assistance with the construction of the apparatus and help with data analysis.

References

[1] For a recent review, see
1995 *Proc. Int. Conf. on Synthetic Metals, (Seoul, 1994); Synth. Met.* **69–71**

[2] Singleton J, Caulfield J, Hill S, Blundell S, Lubczynski W, House A, Hayes W, Perenboom J, Kurmoo M and Day P 1995 *Physica* B **211** 275 and references therein

[3] Harrison N, House A, Deckers I, Caulfield J, Singleton J, Herlach F, Hayes W, Kurmoo M and Day P 1995 *Phys. Rev.* B **52** 5584
[4] Chasseau D, Hebrard S, Hays V, Bravic G, Gautier J, Ducasse L, Kurmoo M and Day P 1995 *Synth. Met.* **70** 947
[5] Recent experimental evidence suggests that the charge is not uniformly distributed amongst the BEDT-TTF ions [6]. This will tend to invalidate previous band-structure calculations which assumed a uniform distribution.
[6] Kepert C J 1996 *PhD Thesis* University of London
[7] Whangbo M H, Ren J, Kang D B and Williams J M 1990 *Mol. Cryst. Liq. Cryst.* **181** 17
[8] Obertelli S D, Marsden I R, Friend R H, Kurmoo M, Rosseinsky M J, Day P, Pratt F L and Hayes W 1990 *Proc. ISSP Int. Symp. on the Physics and Chemistry of Organic Superconductors (Springer Proceedings in Physics 51)* ed G Saito and S Kagomisha (Berlin: Springer) p 181
[9] Mori T and Inokuchi H 1987 *Chem. Lett.* **1987** 1657
[10] Mori T and Inokuchi H 1987 *Solid State Commun.* **64** 335
[11] Kurmoo M, Rosseinsky M J, Day P, Auban P, Kang W, Jerome D and Batail P 1989 *Synth. Met.* **27** A425
[12] Rosseinsky M J, Kurmoo M, Talham D R, Day P, Chasseau D and Watkin D 1988 *J. Chem. Soc. Chem. Commun.* **1988** 88
[13] Seeger K 1974 *Semiconductor Physics* (New York: Springer)
[14] Useful information concerning experimental high-pressure techniques may be found in
Eremets M I 1996 *High Pressure Experimental Methods* (Oxford: Oxford University Press)
[15] Grüner G 1988 *Rev. Mod. Phys.* **60** 1129
[16] Evidence for domain structure in the SDW ground states of a number of BEDT-TTF salts has been observed as hysteresis in the magnetoresistance (see, e.g., references [17, 18, 19])
[17] Athas G J, Brooks J S, Valfells S, Klepper S J, Tokumoto M, Kinoshita N, Kinoshita T and Tanaka Y 1994 *Phys Rev.* B **50** 17 713
[18] Doporto M, Singleton J, Pratt F L, Caulfield J, Hayes W, Perenboom J A A J, Deckers I, Pitsi G, Kurmoo M and Day P 1994 *Phys. Rev.* B **49** 3934
House A, Harrison N, Blundell S J, Deckers I, Singleton J, Perenboom J A A J, Herlach F, Caulfield J, Hayes W and Kurmoo M 1996 *Phys. Rev.* B **53** 9127
[19] Caulfield J, Blundell S J, du Croo de Jongh M S L, Hendriks P T J, Singleton J, Doporto M, House A, Perenboom J A A J, Hayes W, Kurmoo M and Day P 1995 *Phys. Rev.* B **51** 8325
[20] See, e.g.,
Kang W, Hannahs S T and Chaikin P M 1993 *Phys. Rev. Lett.* **70** 3091 and references therein
[21] Sasaki T, Toyota N, Tokumoto M, Kinoshita N and Anzai H 1990 *Solid State Commun.* **75** 93
Sasaki T and Toyota N 1992 *Solid State Commun.* **82** 447
[22] Kepert C J, Frost-Jensen A, Kurmoo M and Day P 1996 in preparation
[23] Ito H, Kartsovnik M V, Ishimoto H, Kono K, Mori H, Kushch N D, Saito G, Ishiguro T and Tanaka S 1995 *Synth. Met.* **70** 899
[24] Fisher M P A 1990 *Phys. Rev. Lett.* **65** 923
[25] Pippard A B 1989 *Magnetoresistance in Metals* (Cambridge: Cambridge University Press)
[26] Caulfield J M 1994 *DPhil Thesis* University of Oxford
[27] Shoenberg D 1984 *Magnetic Oscillations in Metals* (Cambridge: Cambridge University Press)
[28] Everson M P, Johnson A, Lu H-A, Coleman R V and Falicov L M 1987 *Phys. Rev.* B **36** 6953
[29] Caulfield J, Lubczynski W, Pratt F L, Singleton J, Ko D Y K, Hayes W, Kurmoo M and Day P 1994 *J. Phys.: Condens. Matter* **6** 2911
Caulfield J, Lubczynski W, Lee W, Singleton J, Pratt F L, Hayes W, Kurmoo M and Day P 1995 *Synth. Met.* **70** 815
[30] The samples used in reference [11] were prepared in a identical manner to the crystals used in the present work. The data points in figure 7 from reference [11] have been shifted so that the pressure indicated is that at T_1; in the original paper the pressures quoted were measured at a higher temperature [11].
[31] Torrance J B, Bezinge A, Nazzal A I, Huang T C, Parkin S S P, Keane D T, LaPlaca S J, Horn P M and Held G A 1989 *Phys. Rev.* B **40** 8872
[32] Sluchanko N E, Glushkov V V, Demishev S V, Samarin N A, Savchenko A K, Singleton J, Hayes W, Brazhkin V V, Gippius A A and Shulgin A I 1995 *Phys. Rev.* B **51** 1112